Journal of ELECTRICAL ENGINEERING, VOL. 59, NO. 6, 2008, 281–293

A ROBUST DECENTRALIZED POWER SYSTEM LOAD FREQUENCY CONTROL

Hossein Shayeghi *

This paper presents a new robust decentralized controller based on mixed H_2/H_∞ control technique for the solution of Load Frequency Control (LFC) in a deregulated electricity environment. To achieve decentralization in each control area, the connections between this area and the rest of the system and the effects of possible contracts are treated as a set of new disturbance signals. It is shown that, subject to a condition based on the structured singular value (μ), each local area load frequency controller can be designed independently so that stability of the overall closed loop system is guaranteed. In order to minimize effects of load disturbances and to achieve desired level of robust performance in the presence of modeling uncertainties and practical constraints on control action the idea of mixed H_2/H_∞ control technique is being used for the solution of LFC problem. This newly developed design strategy combines advantage of H_2 and H_∞ control syntheses and gives a powerful multi- objectives design addressed by the Linear Matrix Inequalities (LMI) technique. To demonstrate the effectiveness of the proposed method a two-area restructured power system is considered as a test system under different operating conditions. The results of the proposed decentralized controller are compared with the conventional *PI* and pure H_∞ controllers and are shown to minimize the effects of load disturbance and maintain robust performance in the presence of specified uncertainties and system nonlinearities.

K e y w o r d s: LFC, decentralized control, restructured power system, mixed H_2/H_∞ control, robust control, LMI

1 INTRODUCTION

Global analysis of the power system markets shows that the frequency control is one of the most profitable ancillary services at these systems. This service is related to the short-term balance of energy and frequency of the power systems. The most common methods used to accomplish frequency control are generator governor response (primary frequency regulation) and Load Frequency Control (LFC). The goal of LFC is to reestablish primary frequency regulation capacity, return the frequency to its nominal value and minimize unscheduled tie-line power flows between neighboring control areas. From the mechanisms used to manage the provision this service in ancillary markets, the bilateral contracts or competitive offers stand out [1].

In the dynamical operation of power systems, it is usually important to aim for decentralization of control action to individual areas. This aim should coincide with the requirements for stability and load frequency scheduling within the overall system. In a completely decentralized control scheme, the feedback controls in each area are computed on the basis of measurements taken in that area only. This implies that no interchange of information among areas is necessary for the purpose of load frequency control. The advantages of this operating philosophy are apparent in providing cost savings in data communications and in reducing the scope of the monitoring network.

LFC goals, *ie* frequency regulation and tracking the load demands, maintaining the tie-line power interchanges to specified values in the presence of modeling uncertainties, system nonlinearities and area load disturbances determines the LFC synthesis as a multi-objective optimization problem. On the other hand, increasing size and complexity of the restructured power system introduced a set of significant uncertainties and disturbances in power system control and operation, especially on the LFC problem solution. Thus, it is desirable that the novel control strategies be developed to achieve LFC goals and maintain reliability of the electric power system in an adequate level. There have been continuing efforts in design of load frequency controller with better performance according to the change of environment in power system operation under deregulation using various optimal and robust control strategies during the recent years [2–5]. The proposed methods gave good dynamical responses, but robustness in the presence of large modeling uncertainties was not considered and stability of the overall system was not guaranteed. Also, some of them have a centralized scheme which is not feasible for a large power system because of computational and economical difficulties in implementing this scheme.

One of the most important in control theory and application was the direct and inverse Nyquist array methods developed by Rosenbrock and his colleagues [6-8]. The design is based on achieving the required diagonal dominance, so that each control loop can be designed independently. However, it has long been recognized that the main difficulty in applying the Nyquist array method is to obtain the required diagonal dominance (row dominance or column dominance). In particular, if the controller is restricted to be diagonal, the possibility of achieving di-

* Technical Engineering Department, University of Mohaghegh Ardabili Ardebil, Iran, Daneshkah St., P.O.Box: 179, Ardabil, Iran; hshayeghi@gmail.com

ISSN 1335-3632

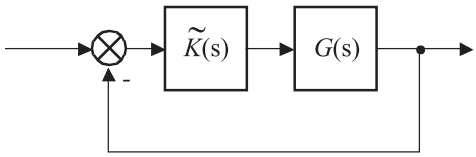

Fig. 1. An equivalent MIMO system

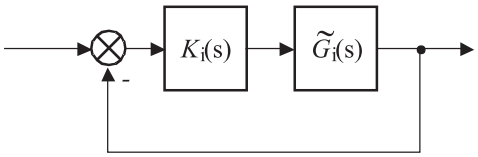

Fig. 2. Independent SISO system design

agonal dominance depends on whether the P-F (Perron-Frobenius) eigenvalues of all the matrices derived from the frequency response magnitudes are less than 2 [7, 9]. As shown in Sec. 5, for the sample system studied in this paper, the above P-F eigenvalue condition is not satisfied.

In this paper to break the limit imposed by the diagonal dominance, the problem of decentralized load frequency controller design is translated into an equivalent problem of decentralized controller design for a Multi-Input Multi-Output (MIMO) control system. It is shown that subject to a condition based on the structured singular values (μ), each local area controller can be designed independently such that stability of the overall closed loop system is guaranteed. The robust stability condition for the overall system can be easily stated as to achieve a sufficient interaction margin, and a sufficient gain and phase margins during each independent design. Based on this framework, a new local robust controller based on the mixed H_2/H_∞ control technique is designed for solution of the LFC problem in a restructured power system. To achieve decentralization, the effects of possible contracted scenarios and connections between each area with the rest of system are treated as a set of new input disturbance signals in each control area. The proposed control strategy combines advantage of H_2 and H_∞ control syntheses to achieve the desired level of robust performance against load disturbances, modeling uncertainties, system nonlinearities and gives a powerful multi-objectives design addressed by the Linear Matrix Inequalities (LMI) techniques [10]. Due to its practical merit, it has a decentralized scheme and requires only the Area Control Error (ACE). When a decentralized LFC is applied, by reducing the system size the resulting controller order will be lower, which is ideally useful for the real world complex power systems.

The proposed control strategy is tested on a two-area power system and compared with the H_∞ controller and PI controller (which is widely used in practical industries). To illustrate effectiveness of the proposed method two scenarios of possible contracts under large load demands have been simulated. The results show that the proposed controller guarantees the robust performance for a wide range of operating conditions in the presence of Generation Rate Constraints (GRC), modeling uncertainties and contract variations.

2 DECENTRALIZED CONTROL DESIGN SCHEME

A centralized controller design is often considered not feasible for large-scale systems such as power system; in turn decentralized control is adopted. The advantages of a decentralized controller design are reduction in the controller complexity and suitability for practical implementation. In the next subsections, the problem of decentralized load frequency controller is translated into an equivalent problem of decentralized control design for a MIMO control system. The proposed method is based on structured singular value (μ).

2.1 Problem formulation

In general, an N-area power system LFC problem can be modeled as a large-scale power system consisting of N subsystems:

$$\begin{aligned} \dot{x} &= A_N x + B_N u\,, \\ y &= C_N x \end{aligned} \tag{1}$$

where $u = [u_1, \ldots, u_N]^\top$; $y = [y_1, \ldots, y_N]^\top$; $x = [x_1, \ldots, x_N]^\top$ and x_i are the state variables for the ith area.

Equivalently, this system composed of N linear time-invariant subsystem $G_i(s)$, described by:

$$\begin{aligned} \dot{x}_i &= A_{ii} x_i + \sum_{j=1 \& j \neq i}^{N} A_{ij} x_j + B_{ii} u_i\,, \\ y_i &= C_{ii} x_i\,. \end{aligned} \tag{2}$$

It assume that all (A_{ii}, B_{ii}) are controllable, (A_{ii}, C_{ii}) are observable and all A_{ii} and C_{ii} are full rank. The term $\sum_{\substack{j=1 \\ j \neq i}}^{N} A_{ij} x_j$ is due to the interconnections to other subsystems. An $N \times N$ transfer function matrix $G(s)$ linking $U(s) = [u_1(s), \ldots, u_N(s)]^\top$ and $Y(s) = [y_1(s), \ldots, y_N(s)]^\top$:

$$Y(s) = G(s)U(s) \tag{3}$$

Can be calculated as:

$$G(s) = C_N (sI - A_N)^{-1} B_N\,. \tag{4}$$

The design of N decentralized local controllers now becomes the design of an $N \times N$ diagonal matrix $\widetilde{K}(s) = \mathrm{diag}\{K_I(s)\}_{i=1,\ldots,N}$ as shown in Figs. 1 and 2.

If all A_{ij} $(i \neq j)$ in $G_i(s)$ were equal to zero, then each controller could be designed by independently just as if it were in a SISO system as shown in Fig. 2. However, since A_{ij} $(i \neq j)$ are not zeros, the following question must be resolved, *ie* if each $K_i(s)$ $(i = 1, \ldots, N)$ is designed to form a stable closed loop system as shown in Fig. 2, what are the additional conditions which can guarantee that the overall system of Fig. 1 is stable? The answer to this question is discussed in the next subsection based on the theorem given by Groshdidier and Morar [11].

2.2 Stability condition

In Groshdidier and Morar's paper, $\widetilde{G}(s)$ is considered as the matrix consisting of the diagonal elements of $G(s)$; *ie*:

$$\widetilde{G}(s)=\mathrm{diag}\{\widetilde{G}_i(s)\}=\mathrm{diag}\{\widetilde{G}_1(s),\widetilde{G}_2(s),\ldots,\widetilde{G}_N(s)\}. \quad (5)$$

Where, $\widetilde{G}_i(s)$ is the ith diagonal element of the transfer function matrix $G(s)$ and has the following state-space realization:

$$\begin{aligned} \dot{x}_i &= A_{ii}x_i + B_{ii}u_i\,, \\ y_i &= C_{ii}x_i\,. \end{aligned} \quad (6)$$

Using the notations:

$$\begin{aligned} &G_d(s) = G(s) - \widetilde{G}(s) \quad E(s) = G_d(s)\widetilde{G}^{-1}(s)\,, \\ &T(s) = G(s)\widetilde{K}(s)\big(I + G(s)\widetilde{K}(s)\big)^{-1}\,, \\ &\widetilde{T}(s) = \widetilde{G}(s)\widetilde{K}(s)\big(I + G(s)\widetilde{K}(s)\big)^{-1} = \mathrm{diag}\big(\widetilde{T}_i(s)\big)\,, \\ &\widetilde{T}_i(s) = K_i(s)\widetilde{G}_i(s)/\big(1 + K_i(s)\widetilde{G}_i(s)\big)\,. \end{aligned} \quad (7)$$

Where, $T(s)$ or $\widetilde{T}(s)$ is a closed loop transfer function matrix for a feedback system consisting of $\widetilde{K}(s)$ and $G(s)$ or $K_i(s)$ and $\widetilde{G}_i(s)$, respectively. Grosdidier and Morar have proved the following theorem:

The closed loop overall system $T(s)$ is stable if:

(c1) – $G(s)$ and $\widetilde{G}(s)$ have the same number of right half-plane poles.

(c2) – The decentralized controller $\widetilde{K}(s)$ stabilizes the diagonal system $\widetilde{G}(s)$.

(c3) – $\sigma_{\max}\big(\widetilde{T}(j\omega)\big) < \mu^{-1}\big(E(j\omega)\big)\ \forall\,\omega$.

Where, $\sigma_{\max}$ denotes the maximum singular value and μ denotes Doyle's structured singular value with respect to the decentralized controller structure of $\widetilde{K}(s)$. Since $\widetilde{T}_i(s)$ is a diagonal matrix in this paper, condition (c3) can be replaced with:

(c3*) $\big|\widetilde{T}_i(j\omega)\big| < \mu^{-1}\big(E(j\omega)\big)\ \forall\,\omega,\ i = 1,\ldots,N$,

where $|\cdot|$ denotes the magnitude.

This theorem gives sufficient conditions for the stability of the overall closed loop system. However, Authors have shown that although (c3*) may has some conservativeness compared with other conditions developed for the independent decoupled design, for example the diagonal dominant condition and the generalized diagonal dominant condition, it gives the tightest restrictive band and is less conservative. However, since the same restriction $\mu^{-1}\big(E(\supset\omega)\big)$ is applied to all $\widetilde{T}_i(s)$ in condition (c3*), a modification on this condition can be made to provide more flexibility and to reduce further the possible conservativeness caused by the inflexibility in condition (c3*):

(c4) $\big|\widetilde{T}_i(j\omega)w_i^{-1}(j\omega)\big| < \mu^{-1}\big(E(j\omega)W(j\omega)\big)\ \forall\,\omega,\ i = 1,\ldots,N$.

Where, $W(s) = \mathrm{diag}\big(w_i(s)\big)_{i=1,\ldots,N}$ is a properly chosen diagonal weighting function matrix. Due to $w_i^{-1}(j\omega)$ in (c-4), although $\mu^{-1}\big(E(j\omega)W(j\omega)\big)$ is still the same for all SISO loops, the restrictions on $\big|\widetilde{T}_i(j\omega)\big|$ are deferent. In fact, (c3*) is a special case of (c4) with $W = I$.

Before applying the above results to our system it is necessary to consider the issue of the robust stability. The stability condition (c4) is given for the nominal plant $G(s)$. If the state space model of Eq. (1) changes, the plant model of $G(s)$ will also change. It is generally not possible to establish a clear relationship between the change of values in Eq. (1) and the change of values involved in condition (c4). For this reason, we specify the robust stability conditions as:

(r1) Condition (c4) is satisfied with a sufficient margin. This can be checked by plotting $\big|\widetilde{T}_I(j\omega)\big|$ and $\mu^{-1}\big(E(j\omega)W(j\omega)\big)|w_i(j\omega)|$ on the same graph and an Interaction Margin (IM) for loop i can be defined as the shortest vertical distance between the two curves.

(r2) There are sufficient gain and phase margins in each SISO loop for the stability. This can also be checked by a Bode or Nyquist plot of $K_i(s)\widetilde{G}_i(s)$.

R e m a r k . For most systems, a satisfactory disturbance rejection performance can be achieved if there are sufficient stability margin.

3 GENERALIZED MODEL OF LFC SCHEME

In the deregulated power systems, the vertically integrated utility no longer exists. However, the common LFC objectives, *ie* restoring the frequency and the net interchanges to their desired values for each control area, still remain. The deregulated power system consists of GENCOs, TRANSCOs and DISCOs with an open access policy. In the new structure, GENCOs may or may not participate in the LFC task and DISCOs have the liberty to contract with any available GENCOs in their own or other areas. Thus, various combinations of possible contracted scenarios between DISCOs and GENCOs are possible. All the transactions have to be cleared by the Independent System Operator (ISO) or other responsible organizations. In this new environment, it is desirable that a new model for LFC scheme be developed to account for the effects of possible load following contracts on system dynamics.

Based on the idea presented in [12], the concept of an *Augmented Generation Participation Matrix* (AGPM) to express the possible contracts following is presented here. The AGPM shows the participation factor of a GENCO in the load following contract with a DISCO. The rows and columns of AGPM matrix equal the total number of GENCOs and DISCOs in the overall power system, respectively. Consider the number of GENCOs and DISCOs in area i be n_i and m_i in a large scale power system with N control areas. The structure of AGPM is given by:

$$AGPM = \begin{bmatrix} AGPM_{11} & \ldots & AGPM_{1N} \\ \vdots & \ddots & \vdots \\ AGPM_{N1} & \ldots & AGPM_{NN} \end{bmatrix}. \quad (8)$$

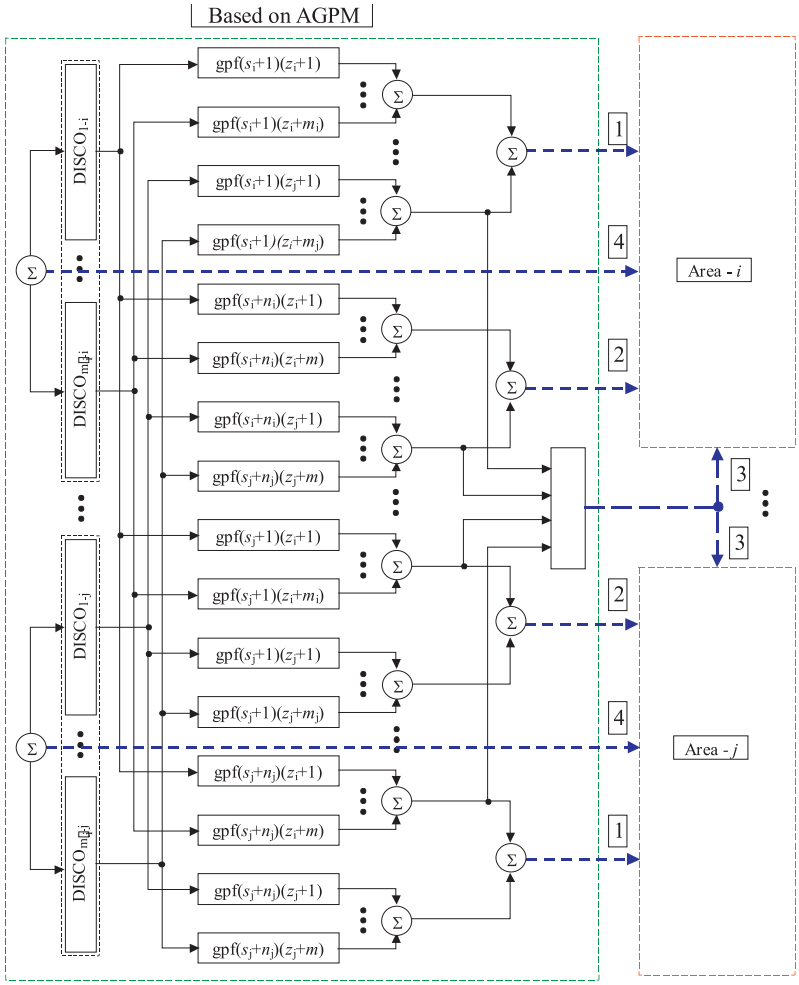

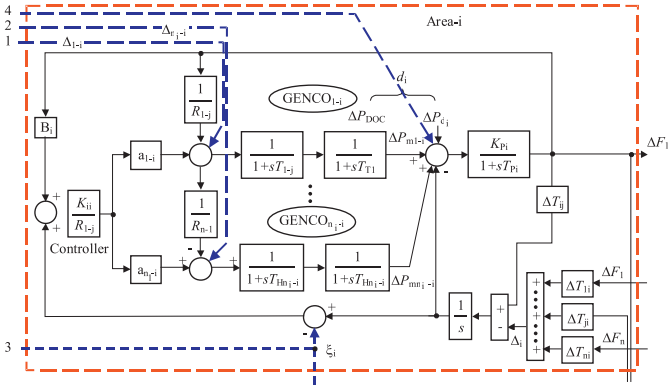

Fig. 3. The generalized LFC scheme in the restructured system

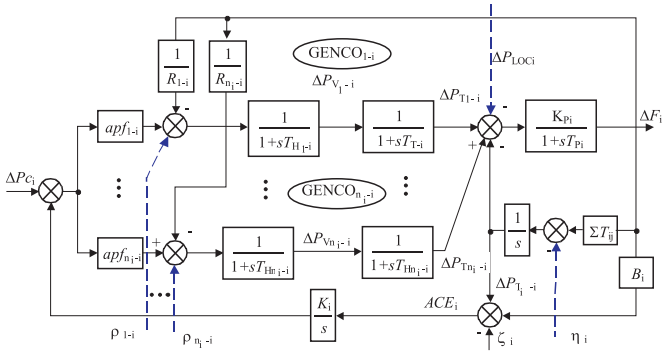

Fig. 4. The decentralized LFC scheme for area i in the restructured environment.

$$AGPM_{ij} = \begin{bmatrix} gpf_{(s_i+1)(z_j+1)} & \cdots & gpf_{(s_i+1)(z_j+m_j)} \\ \vdots & \ddots & \vdots \\ gpf_{(s_i+n_i)(z_j+1)} & \cdots & gpf_{(s_i+n_i)(z_j+m_j)} \end{bmatrix}$$

For $i, j = 1, \ldots, N$ and

$$s_i = \sum_{k=1}^{i-1} n_k\,, \quad z_j = \sum_{k=1}^{i-1} m_k \quad \& \; s_1 = z_1 = 0\,.$$

In the above, gpf_{ij} refers to *generation participation factor* and shows the participation factor of GENCO i in total load following requirement of DISCO j based on the contract. The sum of all entries in each column of AGPM is unity. The diagonal sub-matrices of AGPM correspond to local demands and off-diagonal sub-matrices correspond to demands of DISCOs in one area on GENCOs in another area.

Block diagram of the generalized LFC scheme in a restructured system is shown in Fig. 3. The nomenclature used is given in Appendix A. Dashed lines show interfaces between areas and the demand signals based on the possible contracts. These new information signals are ab-

sent in the traditional LFC scheme. As there are many GENCOs in each area, ACE signal has to be distributed among them due to their ACE participation factor in the LFC task and $\sum_{j=1}^{n_i} \alpha_{ji} = 1$.

Figure 4 shows the modified LFC scheme for control area i in a restructured system. It can be seen from this figure that four input disturbance channels, d_i, η_i, ζ_i and ρ_i are considered for decentralized LFC design. They are defined as bellow:

$$d_i = \Delta P_{Loc,i} + \Delta P_{di}\,,\ \Delta P_{Loc,i} = \sum_{j=1}^{m_i} (\Delta P_{Lj} + \Delta P_{ULj}), \tag{9}$$

$$\eta_i = \sum_{\substack{j=1 \\ j\neq i}}^{N} T_{ij} \Delta f_j\,, \tag{10}$$

$$\zeta_i = \Delta P_{tie,i,sch} = \sum_{\substack{k=1 \\ k\neq i}}^{N} \Delta P_{tie,ik,sch}\,, \tag{11}$$

$$\Delta P_{tie,ik,sch} = \sum_{j=1}^{n_i} \sum_{t=1}^{m_k} apf_{(s_i+j)(z_k+t)} \Delta P_{L(z_k+t)} - \sum_{t=1}^{n_k} \sum_{j=1}^{m_i} apf_{(s_k+t)(z_j+j)} \Delta P_{L(z_i+j)}\,, \tag{12}$$

$$\Delta P_{tie,i-error} = \Delta P_{tie,i-actual} - \zeta_i\,. \tag{13}$$

$$\begin{aligned} \rho_i &= [\rho_{1i} \dots \rho_{ki} \dots \rho_{n_i i}]^\top, \\ \rho_{ki} &= \sum_{j=1}^{N} \Big[\sum_{t=1}^{m_j} gpf_{(s_i+k)(z_j+t)} \Delta P_{Lt-j} \Big], \end{aligned} \tag{14}$$

$$\Delta P_{m,k-i} = \rho_{ki} + apf_{ki} \sum_{j=1}^{m_i} \Delta P_{Ulj-i}\,. \tag{15}$$

$\Delta P_{m,ki}$ is the desired total power generation of a GENCO k in area i and must track the demand of the DISCOs in contract with it in the steady state.

Due to Fig. 4, the state-space model for control area i can be obtained as:

$$\begin{aligned} \dot{x}_i &= A_i x_i + B_{iu} u + B_{iw} w_i'\,, \\ y_i &= C_i x_i + D_{iw} w_i' \end{aligned} \tag{16}$$

where

$$x_i^\top = \big[x_{ai}\ x_{1i} \dots x_{ki} \dots x_{n_i i}\big]\,,\ u_i = \Delta P_{ci},\ y_i = ACE_i\,,$$

$$x_{ai} = \Big[\Delta f_i\ \Delta_{tie,i} \int ACE_i\Big],\ x_{ki} = \big[\Delta P_{Tki}\ \Delta P_{Vki}\big],\quad k = 1, \dots, n_i\,,$$

$$w_i' = \big[\Delta P_{Loc,i}\ \eta_i\ \xi_i\ \rho_i\big],\ \rho_i = \big[\rho_{1i} \dots \rho_{ki} \dots \rho_{n_i i}\big],$$

$$A_i = \begin{bmatrix} A_{11i} & A_{12i} \\ A_{21i} & A_{22i} \end{bmatrix},\ A_{11i} = \begin{bmatrix} 1/T_{Pi} & -K_{Pi}/T_{Pi} & 0 \\ \sum_{\substack{j=1 \\ j\neq i}}^{N} T_{ji} & 0 & 0 \\ B_i & 1 & 0 \end{bmatrix},$$

$$A_{12i} = \underbrace{\left[\begin{pmatrix} K_{Pi}/T_{Pi} & 0 & 0 \\ 0 & 0 & 0 \\ 0 & 0 & 0 \end{pmatrix} \dots \begin{pmatrix} K_{Pi}/T_{Pi} & 0 & 0 \\ 0 & 0 & 0 \\ 0 & 0 & 0 \end{pmatrix} \right]}_{n_i \text{ blocks}}$$

$$A_{21i} = \big[DP_{1i}^\top \dots DP_{ki}^\top \dots DP_{n_i i}^\top\big],$$

$$A_{22i} = \mathrm{diag}(TG_{1i}, \dots, TG_{ki}, \dots, TG_{n_i i})\,,$$

$$DP_{ki} = \begin{bmatrix} 0 & 0 & 0 \\ -1/(R_{ki} T_{Hki}) & 0 & -K_i apf_{ki}/T_{Hki} \end{bmatrix},$$

$$TG_{ki} = \begin{bmatrix} -1/T_{Tki} & 1/T_{Tki} \\ 0 & -1/T_{Hki} \end{bmatrix},$$

$$B_{iu}^\top = \big[0_{3\times 1}^\top\ B_{1iu}^\top \dots B_{kiu}^\top \dots B_{n_i iu}^\top\big],$$

$$B_{kiu} = \big[0\ \ apf_{ki}/T_{Hki}\big],$$

$$B_{iw}^\top = \big[B_{aiw}^\top\ \ B_{1iw}^\top \dots B_{kiw}^\top \dots B_{n_i iw}^\top\big],$$

$$B_{aiw} = \begin{bmatrix} -K_{Pi}/T_{Pi} & 0 & 0 & 0_{1\times n_i} \\ 0 & -1 & 0 & 0_{1\times n_i} \\ 0 & 0 & -1 & 0_{1\times n_i} \end{bmatrix},$$

$$B_{kiw} = \begin{bmatrix} 0_{1\times 3} & 0 & \dots & 0 & \dots & 0 \\ 0_{1\times 3} & b_{1i} & \dots & b_{ki} & \dots & b_{n_i i} \end{bmatrix},$$

$$b_{ji} = \begin{cases} -1/T_{Hki}\,, & j = k\,, \\ 0\,, & j \neq k\,, \end{cases}$$

$$C_i = \big[C_{ai}\ \ 0_{1\times 2n_i}\big],\ \ C_{ai} = \big[B_i\ \ 1\ \ 0\big],$$

$$D_{iw} = \big[0_{1\times 2}\ \ -1\ \ 0_{1\times n_i}\big],$$

4 MIXED H_2/H_∞ AND THE PROPOSED CONTROL FRAMEWORK

This section gives a technical background about the mixed H_2/H_∞ control technique. Also, the proposed synthesis methodology for LFC problem based on the mixed H_2/H_∞ control is given.

4.1 Mixed H_2/H_∞: technical background

In many real world control application, multi objectives such as stability, disturbance attenuation and reference tracking under model uncertainties and practical constraints are followed simultaneously. On the other hand, each robust control method is mainly useful to capture a set of special design specifications. For instance, noise attenuation or regulation against random disturbances is more naturally expressed in LQG terms (H_2 synthesis). Similarly, pure H_∞ synthesis is more useful for holding close-loop stability and formulation of some uncertainties and practical control constraints. It is shown that combination of H_2 and H_∞ (mixed H_2/H_∞) control techniques gives a powerful multi-objectives design including both sets of the above objectives. The synthesis problem is shown in Fig. 5. $P(s)$ is a linear time invariant system with the following state-space realization:

$$\begin{aligned} \dot{x} &= Ax + B_1 w + B_2 u\,, \\ z_\infty &= C_\infty x + D_{\infty 1} w_i + D_{\infty 2} u\,, \\ z_2 &= C_2 x + D_{21} w_i + D_{22} u_i\,, \\ y_i &= C_y x + D_{y1} w_i\,. \end{aligned} \tag{17}$$

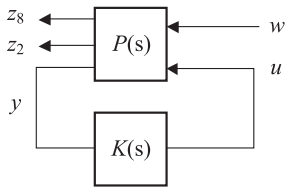

Fig. 5. The mixed H_2/H_∞ synthesis structure

Where, x is the state variable vector, w is the disturbance and other external vector and y is the measured output vector. The output channels z_∞ is associated with the H_∞ performance, while the output channel z_2 is associated with the H_2 performance.

Denoting by $T_\infty(s)$ and $T_2(s)$, the transfer functions from w to z_∞ and z_2, respectively, the mixed H_2/H_∞ synthesis problem can be expressed by the following optimization problem: design a controller $K(s)$ that minimize a trade off criterion of the form:

$$\alpha\|T_\infty(s)\|^2 + \beta\|T_2(s)\|^2 \quad (\alpha\,\&\,\beta \geq 0)\,. \tag{18}$$

An efficient algorithm for solving this problem is available in LMI control toolbox of MATLAB [13]. The following lemmas relate the above optimization control problem to LMI techniques. Assume that the state-space realization of close loop system is given by as:

$$\begin{aligned} \dot{x}_{cl} &= A_{c1}x_{c1} + B_{c1}w\,,\\ z_\infty &= C_{cl\infty}x_{cl} + D_{cl\infty}w\,,\\ z_2 &= C_{cl2}x_{cl} + D_{cl2}w\,. \end{aligned} \tag{19}$$

LEMMA 1 (H_∞ performance) [14]. *The closed loop RMS gain for $T_\infty(s)$ does not exceed γ_∞ if and only if there exist a symmetric matrix $X_\infty > 0$ such that:*

$$\begin{bmatrix} A_{cl}X_\infty + X_\infty A_{cl}^\top & B_{cl} & X_\infty C_{cl}^\top \\ B_{cl}^\top & -I & D_{cl\infty}^\top \\ C_{cl\infty}X_\infty & D_{cl\infty} & -\gamma_\infty^2 I \end{bmatrix} < 0\,. \tag{20}$$

LEMMA 2 (H_2 performance) [14]. *The H_2 norm of $T2(s)$ does not exceed γ_2 if and only if $D_{cl2} = 0$ and here exist two symmetric matrices X_2 and Q such that:*

$$\begin{bmatrix} A_{cl}x_2 + X_2A_{cl}^\top & B_{cl} \\ B_{cl}^\top & -I \end{bmatrix} < 0\,,\ \begin{bmatrix} Q & C_{cl2}X_2 \\ X_2C_{cl2}^\top & X_2 \end{bmatrix} > 0\,,\ \operatorname{trace}(Q) < \gamma_2^2\,. \tag{21}$$

4.2 LFC problem formulation via Mixed H_2/H_∞

LFC goals, *ie* frequency regulation and tracking the load demands, maintaining the tie-line power interchanges to specified values in the presence of modeling uncertainties, system nonlinearities and area load disturbances determines the LFC synthesis as a multi-objective optimization problem. For this reason, the idea of mixed H_2/H_∞ control synthesis, which gives a powerful multi-objectives design is used for solution this problem. The main synthesis framework to formulate it as a mixed H_2/H_∞ control design for a given control area (Fig. 4) is shown in Fig. 6.

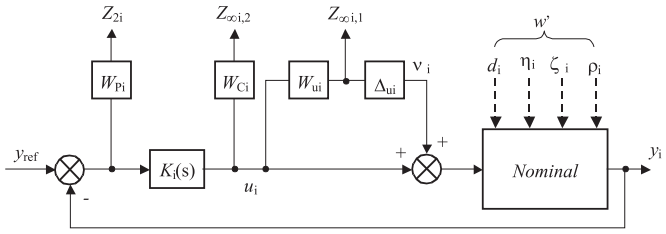

Fig. 6. The proposed synthesis framework

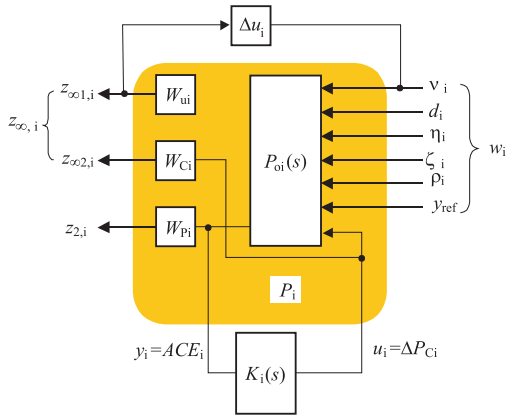

Fig. 7. The formulation of mixed H_2/H_∞ based control design problem

In the power systems, each control area contains different kinds of uncertainties because of plant parameter variations, load changes and system modeling errors due to some approximations in model linearization and unmodeled dynamics. Usually, the uncertainties in power system can be modeled as multiplicative and/or additive uncertainties [15]. In Fig. 6 the Δu_i block models the structured uncertainties as a multiplicative type and W_{ui} is the associated weighting function. The output channels $z_{\infty i,1}$ and $z_{\infty i,2}$ are associated with H_∞ performance. The first channel is used to meet robustness against uncertainties and reduce their impacts on close loop system performance. In the second channel ($z_{\infty i,2}$) W_{Ci} sets a limit on the allowed control signal to penalize fast change and large overshoot in the control action signal with regard to practical constraints. The output channel z_{2i} is associated with the H_2 performance and W_{Pi} sets the performance goal *ie* zero tracking error and minimizing the effects of disturbances on the area control error (ACE_i). We can redraw the Fig. 6 as a mixed H_2/H_∞ general framework synthesis as shown in Fig. 7, where $P_{oi}(s)$ and $K_i(s)$ denote the nominal area model as given by Eq. (16) and controller, respectively. Also,

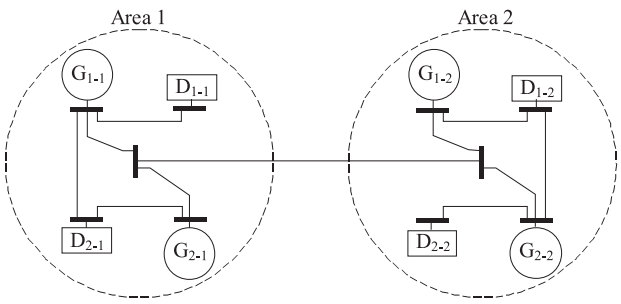

Fig. 8. Two area control power system

Table 1. GENCOs parameters

MVA_{base} (1000 MW)	GENCOs (k in area i)			
Parameter	1-1	2-1	1-2	2-2
Rate (MW)	1000	800	1100	900
T_T (sec)	0.3	0.3	0.3	0.3
T_H (sec)	0.1	0.1	0.1	0.1
R (Hz/pu)	2.4	3.3	2.5	2.4
α	0.75	0.25	0.5	0.5

Table 2. Control area parameters

Parameter	Area-1	Area-2
T_p (sec)	20	20
K_p	120	120
R (Hz/pu)	2.4	2.4
B (pu/Hz)	0.425	0.425
K_I	0.12	0.12
T_{ij} (pu/Hz)	$T_{12} = T_{21} = 0.545$	

y_i is the measured output (performed by ACE_i), u_i is the control output and w_i includes the perturbed, disturbance and reference signals in the control area.

In Fig. 7, $P_i(s)$ is the Generalized Plant (GP) that includes nominal models of control area i and associated weighting functions. The state-space model of GP can be obtained as:

$$\begin{aligned} \dot{x}_{Api} &= A_{Gpi}x_{Gpi} + B_{1i}w_i + B_{2i}u_i\,, \\ z_{\infty i} &= C_{\infty i}x_{Gpi} + D_{\infty 1i}w_i + D_{\infty 2i}u_i\,, \\ z_{2i} &= C_{2i}x_{Gpi} + D_{21i}w_i + D_{22i}u_i\,, \\ y_i &= C_{yi}x_{Gpi} + D_{y1i}w_i \end{aligned} \tag{22}$$

$$w_i^\top = \begin{bmatrix} v_i & d_i & \eta_i & \zeta_i & \rho_i & y_{ref} \end{bmatrix},\ z_{\infty i}^\top = \begin{bmatrix} z_{\infty 1i} & z_{\infty 2i} \end{bmatrix}.$$

Now, the synthesis problem is: designing a controller $K_i(s)$ as shown in Fig. 7 such that Eq. (18) is minimized. It is should be noted that the order of found controller by this strategy is the same as size of generalized plant that is typically high in general. In order to overcome the complexity of computation in the case of high order power systems, appropriated model reduction techniques might be applied to the obtained controller model. In summery, the designing steps of the proposed method are:

Step 1: Formulation of the LFC problem as a decentralized control scheme due to Fig. 4 and identify the state space model for the given control area.

Step 2: Identify the uncertainty (W_{ui}) and performance weighting functions (W_{Pi} and W_{Ci}) for the given area according to dynamical model, practical limits and performance requirements.

Step 3: Problem formulation as a general mixed H_2/H_∞ control structure according to Fig. 7.

Step 4: Identify the indexes α, β and solve optimization problem Eq. (18) using LMI approaches to obtain desired controller.

Step 5: Reduce the order of result controller by using standard model reduction techniques.

Step 6: Continue this procedure by applying the above steps to other control area.

Step 7: Retune the obtained decentralized controller to best performance and check if the overall power system satisfies the robust stability condition as given in Sec. 2 and has enough IM, gain and phase margins.

The proposed control methodology in this paper includes enough flexibility to set the desired level of robust performance and provides a set of robust decentralized controllers which guarantee stability of the overall power system. On the other hand, it has a decentralized scheme and requires only the ACE in each control area. Thus, its construction and implementation are easy and can be useful in the real world complex power system.

5 CASE STUDY

A two-area power system, shown in Fig. 8 is considered as a test system to demonstrate the effectiveness of the proposed control strategy. It is assumed that each control area includes two GENCOs and two DISCOs. The power system parameters are given in Tables 1 and 2. According to problem formulation given in Sec. 2, the state-space realization of the overall system can be constructed as:

$$\begin{aligned} \dot{x} &= Ax + Bu\,, \\ y &= Cx\,. \end{aligned} \tag{23}$$

Where, $u = [u_1 \ \ u_2]^\top$; $y = [y_1 \ \ y_2]^\top = [ACE_1 \ \ ACE_2]^\top$; $x = [x_1 \ \ x_2]^\top$ and x_i is the state variable for ith area as given in Eq. (16), $A \in R^{14\times 14}$, $B \in R^{14\times 2}$, $C \in R^{2\times 14}$.

$$A = \begin{bmatrix} A_{11} & A_{22} \\ A_{21} & A_{22} \end{bmatrix},$$

$$B = \text{blockdiagonal}\big(B_{11}, B_{22}\big);$$

$$C = \text{blockdiagonal}\big(C_{11}, C_{22}\big)\,.$$

A_{ii}, B_{ii} and C_{ii} are the same as A_i, B_{iu}, C_i as given in Eq. (16). The A_{ij} is given by:

$$A_{ij} = \big[a_{ij}\big]_{i=1,\ldots,n_i;\, j=1,\ldots,n_j}\,.$$

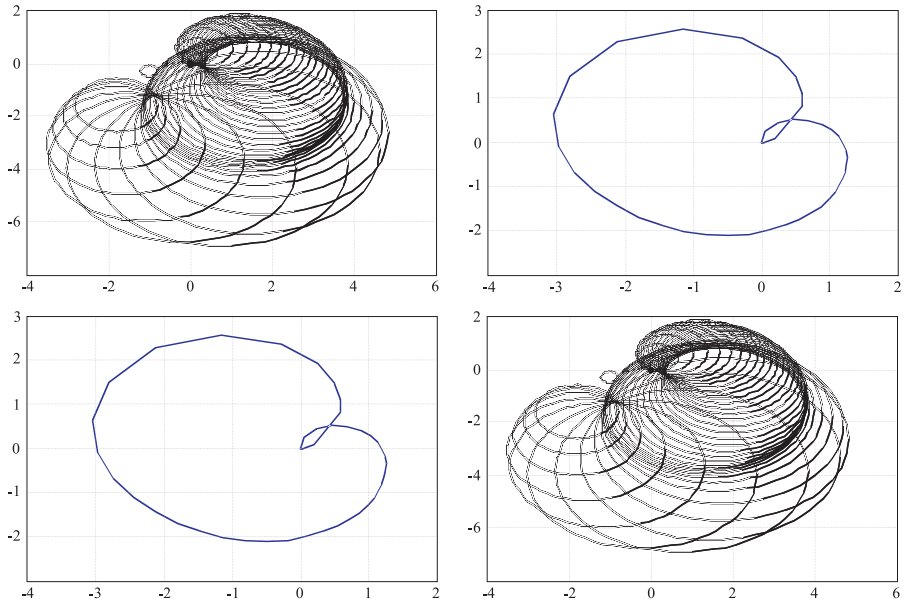

Fig. 9. Nyquist array with the column Gershgorin circles

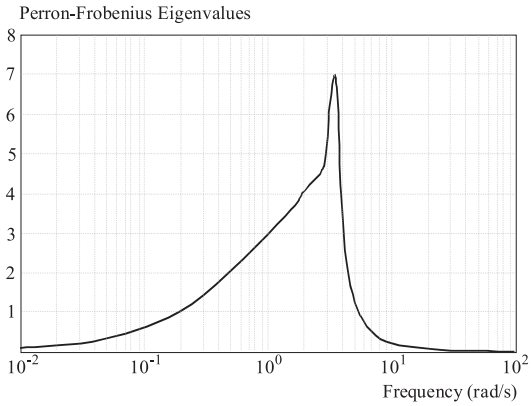

Fig. 10. P-F eigenvalues for the $G(s)$

Where, n_i and n_j are the number of state variables area i and j, respectively and for the given sample system n_1 and n_2 are 7. The all entries of a_{ij} is zero except the a_{21} is $-T_{ij}$.

A 2×2 transfer function matrix for the system can be obtained as $G(s) = C(sI - A)^{-1}B$. A Nyquist array with the column Gershgorin circles on the diagonal elements is plotted in Fig. 9. The frequency responses of diagonal elements with the Gershgorin circles enclose the origin of the complex plane. This show that the system is not diagonal dominant. The P-F eigenvalues related to the $G(s)$ are depicted in Fig. 10 which shows that it is impossible to use a diagonal compensator to achieve the required diagonal dominance. It is therefore also not possible to use the Nyquist array method to design the required decentralized controller [9].

To break the limit imposed by the diagonal dominance, the design method proposed in this paper is applied here. Simulation results and eigenvalue analysis show that the open loop system performance is affected more significantly by changing in the K_{pi}, T_{pi}, B_i and T_{ji} than changes of other parameters [16]. Thus, to illustrate the capability of the proposed strategy in this example, in the view point of uncertainty our focus will be concentrated on variation of these parameters. Hence, for the given power system, we have set our objectives to area frequency regulation and assuring robust stability and performance in the presence of specified uncertainties, load disturbances or exogenous inputs as follows:

1. Holding stability and robust performance for the overall power system and each control area in the presence of 25 % uncertainty for the K_{pi}, T_{pi}, B_i and T_{ji}.
2. Minimizing the effects of new introduced disturbances on the output signals according to the possible contracts and area interface $(\eta_i, \zeta_i, \rho_i)$.
3. Getting zero steady state error and good tracking for load demands and disturbances.
4. Maintaining acceptable overshoot and settling time on the frequency deviation signal in each control area.
5. Setting the reasonable limit on the control action signal from the change speed and amplitude view point.

Following, we will discuss application of the proposed strategy on the given power system to achieve the above objectives.

5.1 Uncertainty weights selection

As it is mentioned in the previous section, we can consider the specified uncertainty in each area as a multiplicative uncertainty associated with a nominal model. Let $\widehat{P}_i(s)$ denote the transfer function from the control input u_i to control output y_i at operating points other than the nominal point. Following a practice common in robust control, this transfer can be represented as:

$$\left|\Delta u_i(s) W_i(s)\right| = \left(\widehat{P}_i(s) - P_{oi}(s)\right)/P_{oi}(s)\big|;\ P_{oi}(s) \neq 0\,,$$
$$\left\|\Delta u_i(s)\right\|_\infty = \sup\left|\Delta u_i(s)\right| \leq 1\,. \qquad (24)$$

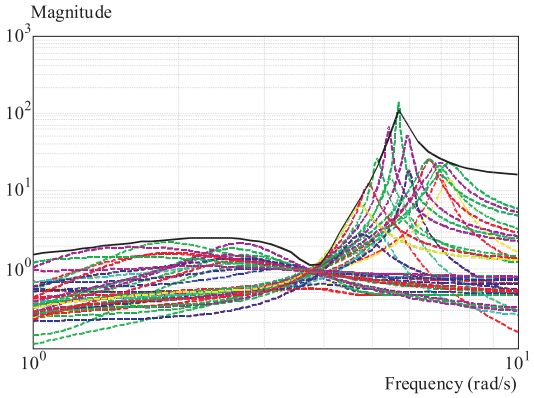

Fig. 11. Uncertainty plot due to change of K_{P1}, T_{P1}, B_1 and T_{j1} (Dashed) and $W_{u1}(s)$ (Solid)

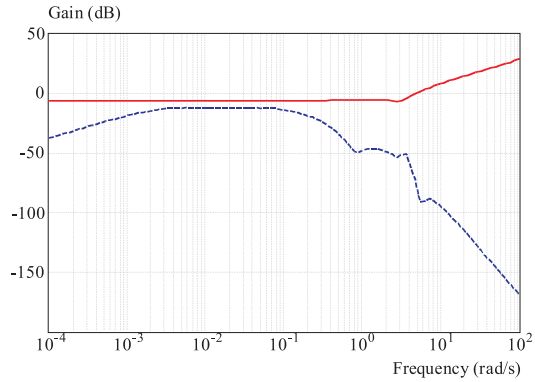

Fig. 13. Plot of $\mu^{=1}(E(j\omega))$ and $\widetilde{T}_1(s)$

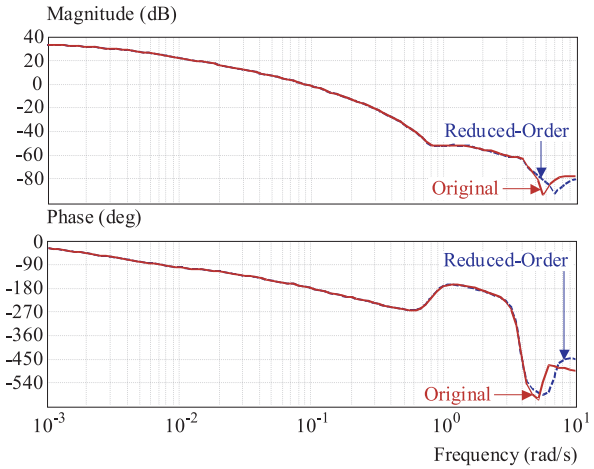

Fig. 12. Bode plot comparison of original and reduced order controller $K_{1mix}(s)$

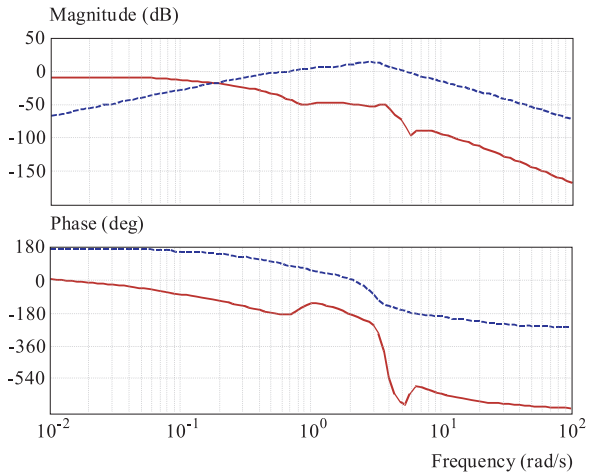

Fig. 14. Bode plot of $K_1(s)\widetilde{G}_1(s)$ (Solid) and $\widetilde{G}_1(s)$ (Dashed)

Where, $\Delta u_i(s)$ shows the uncertainty block corresponding to the uncertain parameters and $P_{oi}(s)$ is the nominal transfer function model. Thus, $W_{ui}(s)$ is such that its magnitude Bode plot covers the Bode plot of all possible plants. Using Eq. (24) some sample uncertainties corresponding to different values of K_{pi}, T_{pi}, B_i and T_{ji} are shown in Fig. 11 for one area. It can be seen that multiplicative uncertainties have a peak around the 5.5 rad/s. Based on this figure the following multiplicative uncertainty weight was chosen for control design as:

$$W_{u1} = \frac{14.3s^3 + 8.2s^2 + 213.8s + 10.39}{s^3 + 4.18s^2 + 33.84s + 125.41}. \qquad (25)$$

Figure 11 clearly shows that attempting to cover the sharp peak around the 5.5 rad/s will result in large gaps between the weight and uncertainty at other frequencies. On the other hand, a tighter fit at all frequencies using a high order transfer function will result in a high order controller. The weight (25) used in our design give a conservative design at around the 5.5 rad/s, low and high frequencies, but it provides a good trade off between robustness and controller complexity. Using the same method, the uncertainty weighting function for area 2 are also calculated which is identical with weighting function of area 1.

5.2 Performance weights selection

The selection of performance weights W_{Ci} and W_{Pi} entails a trade off among different performance requirements, particularly good area control error minimization versus peak control action. The weight on the control input, W_{Ci}, must be chosen close to a differentiator to penalize fast change and large overshoot in the control input due to corresponding practical constraints. The weight on the output, W_{Pi}, must be chosen close to an integrator at low frequency in order to get disturbance rejection and zero steady state error. More details on how these weights are chosen are given in [17, 18]. Based on the above discussion, a suitable set of performance weighting functions for one control area is chosen as:

$$W_{C1} = \frac{0.3s + 1}{s + 10}, \quad W_{P1} = \frac{0.03s + 0.75}{350s + 1}. \qquad (26)$$

5.3 Pure H_∞ control design

In addition to the proposed control strategy, a pure H_∞ dynamic controller is developed using Lemma 1. Specifically, the control design is reduced to an LMI formulation, and then, the H_∞ control problem is solved according to the LMI constrain (20) using the function *hinflmi* provided by MATLAB's LMI control toolbox [13]. The same control framework (shown in Fig. 7) is used for

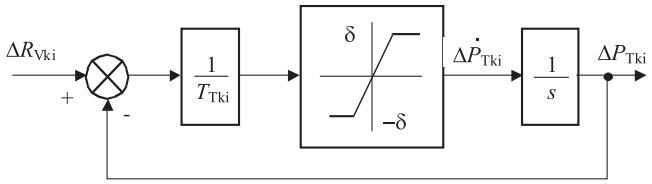

Fig. 15. A nonlinear turbine model with GRC.

Table 3. Gain and phase margins.

		Loop 1 (Area-1)		Loop 2 (Area-2)	
		GM (dB)	PM (deg)	GM (dB)	PM (deg)
$\widetilde{G}_1(s)$		6.01	15.7	6.01	15.7
$K_i(s)\widetilde{G}_i(s)$	H_∞	27.6	∞	27.6	∞
	Mixed	45.51	∞	45.51	∞

the pure H_∞ control design but using only one fictitious output channel (Z_∞) as:

$$Z_{\infty i}^{\top} = \left[Z_{\infty 1i} \;\; Z_{\infty 2i} \;\; Z_{2i} \right]. \tag{27}$$

The resulting controller is dynamic type and whose order is the same as the size of GP model (here 12). The order of controller is reduced to a 6 using the standard Hankel norm approximation and is given as follows:

$$\begin{aligned} K_{1\infty} &= 2.17 \times 10^{-3} \frac{N(s)}{D(s)}, \\ N(s) &= s^5 + 15.77s^4 + 38.23s^3 + 348.45s^2 \\ &\quad + 70.63s + 11.29, \\ D(s) &= s^6 + 1.995s^5 + 16.039s^4 + 19.507s^3 \\ &\quad + 6.865s^2 + 0.433s + 0.0029. \end{aligned} \tag{28}$$

5.4 Mixed H_2/H_∞ control design

Based on the problem formulation and synthesis methodologies in Sec. 4, a decentralized robust controller is designed for one control area using the *hinfmix* function in the LMI control toolbox. This function gives an optimal controller through the mentioned optimization problem Eq. (18) with α and β fixed at unity. The resulting controller is dynamic type and whose order is the same as the size of the GP model (here 12). The controller is reduced to a 5 order with no performance degradation using the standard Hankel norm approximation. The Bode plots of the full order and reduced order controllers are shown in Fig. 12. The transfer function of the reduced order controller with simple structure is given as:

$$K_{1mis}(s) = 4.72 \times 10^{-3} \times \frac{s^4 - 2.242s^3 + 12.88s^2 + 0.963s + 8.889}{s^5 + 4.7o3s^4 + 10.146s^3 + 4.7262s^2 + 0.321s + 0.0009}. \tag{29}$$

Using the same procedure and setting similar objectives as discussed above the set of suitable weighting function for the other control area synthesis is chosen as same as area 1. The transfer function of resulting controller is identical with transfer function of controller area 1.

5.5 Stability analysis

In this subsection, stability of the overall system with proposed decentralized mixed H_2/H_∞ based controller is investigated. Due to discussion as mentioned in Sec. 2. and choosing the weighting function W as a unity matrix, a plot of $\mu^{-1}\big(E(j\omega)\big)$ and the magnitude frequency response of $\widetilde{T}_1(s)$ are depicted in Fig. 13. From this figure, the IM defined before for area 1 is: 5.2 dB at $\omega = 0.016$ rad/s. The frequency response of $\widetilde{T}_2(s)$ is the same as $\widetilde{T}_1(s)$ and therefore the IM for area 2 is identical with area 1. The frequency response of $\widetilde{G}_1(s)$ and $K_1(s)\widetilde{G}_1(s)$ is shown in Fig. 14. The GM is increased from 6.01 to 45.51 dB and the PM is increased from 15.7° to infinity. The improvements each individual loop's GM and PM are listed in Table 3 for two areas.

The above results show that when the frequency response based diagonal dominance cannot be achieved, the condition based on the structured singular value can be applied to design decentralized controller for the required system performance and guaranteeing stability of the overall system.

6 SIMULATION RESULTS

In order to illustrate the behavior of the proposed control strategy some simulations has been carried out. In the simulation study, the linear model of a turbine $\Delta P_{Vki}/\Delta P_{Tki}$ in Fig. 3 for each GENCO is replaced by a nonlinear model of Fig. 15 (with ± 0.03 limits). This is to take GRC into account *ie* the practical limit on the area of change in the generating power of each GENCO. It is noted that GRC would influence the dynamic responses of the system significantly and lead to longer overshoot and longer settling time.

The close loop system performance using the proposed mixed H_2/H_∞ based controller in comparison with the pure H_∞ PI controllers (which is widely used for LFC problem in industry) controllers is tested for two cases of operating conditions in the presences of load demands, disturbances and uncertainties.

6.1 Scenario 1

In this scenario, the closed loop performance is tested in the presence of both step contracted load demands and uncertainties. It is assumed that a large step load 0.1 pu MW is demanded by all DISCOs. A case of combined Poolco and bilateral based contracts between DISCOs and available GENCOs is considered based on the following AGPM:

$$AGPM = \begin{bmatrix} 0.5 & 0.25 & 0 & 0.3 \\ 0.2 & 0.25 & 0 & 0 \\ 0 & 0.25 & 0 & 0.7 \\ 0.3 & 0.25 & 0 & 0 \end{bmatrix}$$

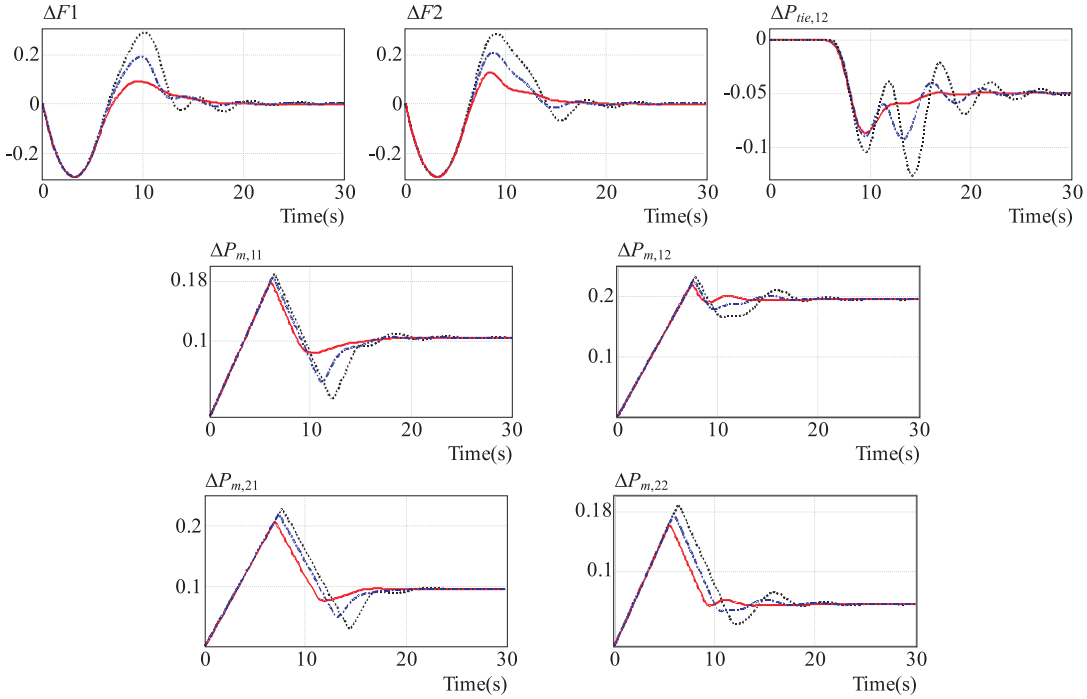

Fig. 16. Power system response to scenario 1 a) Frequency deviation and tie line power changes b) GENCOs Power changes; Solid (Mixed), Dashed-dotted (H_∞) and Dotted (PI)

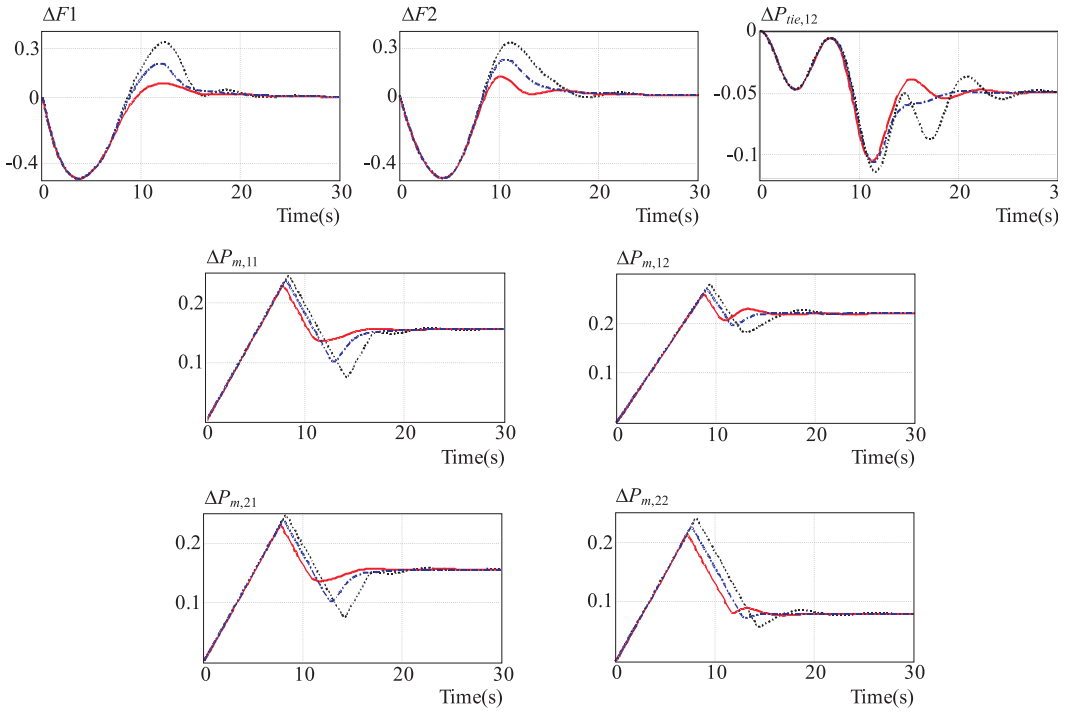

Fig. 17. Power system response to scenario 2 a) Frequency deviation and tie line power changes b) GENCOs Power changes; Solid (Mixed), Dashed-dotted (H_∞) and Dotted (PI)

All GENCOs participate in the LFC task. The GENCO 2 in area 1 only participate for performing the LFC in its area, while other GENCOs track the load demand in their areas and/or others. Power system responses with 25 % increase in uncertain parameters K_{Pi}, T_{Pi}, B_i and T_{ij} are depicted in Fig. 16. Using the proposed method, the frequency deviation of two areas is quickly driven back to zero and the tie-line power flows properly converges to the specified values of Eq. (12) in the steady state. *ie*: $\Delta P_{tie,1,sch} = -0.05$ pu MW.

The actual generated powers of GENCOs properly reached the desired values in the steady state as given

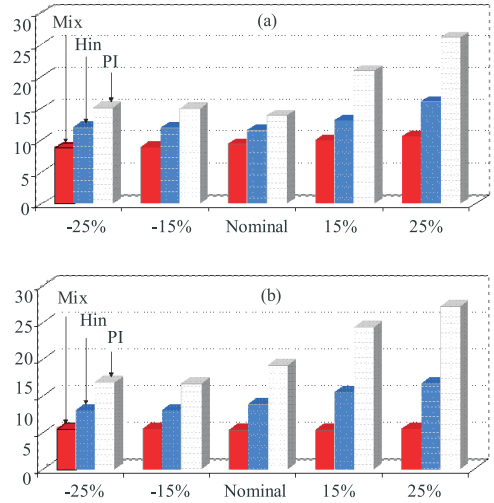

Fig. 18. Values of performance indices under scenario 1: a) ITAE b) FD

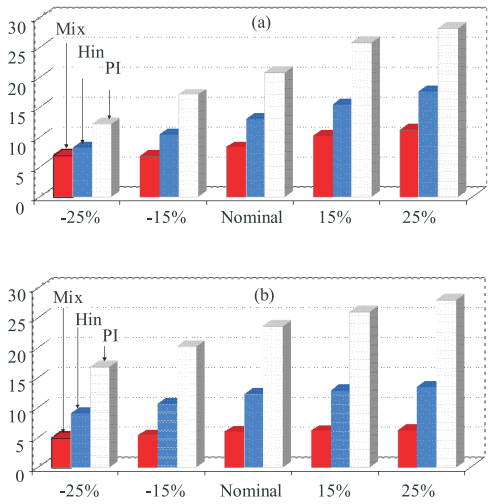

Fig. 19. Values of performance indices under scenario 2: a) ITAE b) FD

by Eq. (15). *ie*:

$$\Delta P_{m,1-1} = 0.105\,, \qquad \Delta P_{m,2-1} = 0.045\,\text{pu MW},$$
$$\Delta P_{m,1-2} = 0.195\,, \qquad \Delta P_{m,2-2} = 0.055\,\text{pu MW}.$$

6.2 Scenario 2

In this case, a DISCO may violate a contract by demanding more power than that specified in the contract. This excess power is reflected as a local load of the area (un-contracted load). Consider scenario 1 again. It is assumed that in addition to specified contracted load demands and 25 % decrease in uncertain parameters, the one DISCO from areas 1 and 2 demand 0.1 and 0.05 pu MW as a large un-contracted load, respectively. Using the Eq. (9), the total local load in all areas is obtained as:

$$\Delta P_{Loc,1} = 0.3\,, \quad \Delta P_{Loc,2} = 0.25\,\text{pu MW}.$$

The purpose of this scenario is to test the effectiveness of the proposed controller against uncertainties and large load disturbances in the presence of GRC. The power system responses are shown in Fig. 17.

Using the proposed method, the frequency deviation of these areas is quickly driven back to zero and the tie-line power flows properly converge to the specified value of Eq. (12) in the steady state. As AGPM is the same as in scenario 1 and the un-contracted load of areas is taken up by the GENCOs in the same areas, the tie-line power is the same as in scenario 1 in the steady state (Fig. 17). The un-contracted load of DISCOs in area 1 and 2 is taken up by the GENCOs in these areas according to ACE participation factors in the steady state. Using the Eq. (15) the actual generated power of GENCOs is given by:

$$\Delta P_{m,1-1} = 0.155\,, \qquad \Delta P_{m,2-1} = 0.095\,\text{pu MW},$$
$$\Delta P_{m,1-2} = 0.22\,, \qquad \Delta P_{m,2-3} = 0.08\,\text{pu MW},$$

As shown in Figs. 17-b and c, the actual generated powers of GENCOs properly reached the desired values using the proposed strategy. The simulation results in the above scenarios indicate that the proposed control strategy can ensure the robust performance such as frequency tracking and disturbance attenuation for possible contracted scenarios under modeling uncertainties and large area load demands in the presence of GRC.

To demonstrate robust performance of the proposed control strategy, the performance indices Integration-Time-Absolute-Error (ITAE) based on ACE and Figure of Demerit (FD) based on system performance characteristics (suitably weighted) is being used as:

$$ITAE = \int_0^{30} t\big(|ACE_1(t)| + |ACE_2(t)\big)\mathrm{d}t\,,$$
$$FD = (OS \times 15)^2 + (US \times 5)^2 + 0.1 \times T_s)^2. \tag{30}$$

Overshoot (OS), undershoot (US) and settling time (for 5 % band of the total step load demand in area 1) of frequency deviation area 1 are considered for evaluation of FD. The values of ITAE and FD are calculated for the above two scenarios whereas the uncertain parameters of system are varied from $-25\,\%$ to $25\,\%$ of the nominal values. Figures 18-19 show the values of ITAE and FD for operation conditions under scenarios 1-2, respectively.

It can be seen that in comparison with both PI and H_∞ controllers, the mixed H_2/H_∞ controller designed in this paper is very effective and significantly improves the system performance against the plant parameters changes.

7 CONCLUSION

A new decentralized robust load frequency controller in the competitive electricity environment using the generalized LFC scheme model for accounting the effects of the possible load following contracts is proposed in this paper. It is shown that, when the frequency response

based diagonal dominance can not be achieved, subject to a condition based on the structured singular values (μ), each local area controller can be designed independently such that stability of the overall system is guaranteed. Since, each control area contains different kinds of uncertainties and disturbances because of increasing the complexity and change of power system structure. Thus, the LFC problem has been formulated as a decentralized multi-objective optimization control problem via a mixed H_2/H_∞ control approach and solved by LMI techniques to obtain optimal controller. Synthesis problem introduce appropriate uncertainties to consider of practical limits, has enough flexibility for setting the desired level of robust performance and leads to a set of relatively simple controllers, which are ideally practical for the real world complex power systems.

The effectiveness of the proposed strategy was tested on a three-area power system and compared with the H_∞ and PI controllers under possible contracts with various load changes in the presence of modeling uncertainties and GRC. The simulation results show that the proposed method achieves good robust performance such as frequency regulation, tracking the load changes and disturbances attenuation for a wide range of plant parameter changes and area load conditions. The system performance characteristics in terms of 'ITAE' and 'FD' indices reveal that the proposed robust controller is a promising control scheme for the solution of LFC problem and therefore it is recommended to generate good quality and reliable electric energy in the restructured power systems.

Appendix A: Nomenclature

F	area frequency
P_{Tie}	net tie-line power flow
P_T	turbine power
P_V	governor valve position
P_C	governor set point
ACE	area control error
apf	ACE participation factor
Δ	deviation from nominal value
K_P	subsystem equivalent gain
T_P	subsystem equivalent time constant
T_T	turbine time constant
T_H	governor time constant
R	droop characteristic
B	frequency bias
K	Gain of integral controller
T_{ij}	tie line synchronizing coefficient between areas i and j
P_{Lj-i}	contracted demand of Disco j in area i
P_{ULj-i}	un-contracted demand of Disco j in area i
$P_{m,j-i}$	Power generation of GENCO j in area i
P_{Loc}	Total local demand
η	area interface
ζ	scheduled power tie line power flow deviation ($\delta P_{tie,sch}$)

References

[1] RAINERI, R.—RIOS, S.—SCHIELE, D.: Technical and Economic Aspects of Ancillary Services Markets in the Electric Power Industry: an International Comparison, Energy Policy **34** No. 13 (2006), 1540–1555.

[2] FELIACHI, A.: On Load Frequency Control in a Deregulated Environment, In: Proceedings of the IEEE International Conference on Control Applications, 15-18 Sept. 1996, pp. 437–441.

[3] RERKPREEDAPONG, D.—HASANOVIC, A.—FELIACHI, A.: Robust Load Frequency Control Using Genetic Algorithms and Linear Matrix Inequalities, IEEE Trans. On Power Systems **18** No. 2 (2003), 855–861.

[4] LIU, F.—SONG, Y. H.—MA, J.—LU, Q.: Optimal Load Frequency Control in Restructured Power Systems, IEE Proc. Gener. Transm. Distrib. **150** No. 1 (2003), 87–95.

[5] BEVRANI, H.—MITANI, Y.—TSUJI, K.: Robust Decentralized AGC in a Restructured Power System, Energy Conversion and Management **45** No. 15-16 (2004), 2297–2312.

[6] ROSENBROCK, H. H.: Computer Aided Control System Design, Academic Press, 1974.

[7] MUMRO, N.: Recent Extensions to the Inverse Nyquist Array Design Method, Proc. of 24$^{\text{th}}$ CDC Conference, 1985, pp. 1852–1857.

[8] MUMRO, N.—EDMUNDS, J. M.: The Inverse Nyquist Array and Characteristic Locus Design Methods, In: The Control Handbook (Levine,W.S., ed.), CRC/IEEE Press, 1996.

[9] MEES, A. I.: Achieving Diagonal Dominance, Syst. and Cont. Lett. **1** (1981), 155–158.

[10] SCHERER, C.—GAHINET, P.—CHILALI, M.: Multi-Objective Output-Feedback Control via LMI Optimization IEEE, Trans. On Automatic Control **42** No. 7 (1997), 896–911.

[11] GROSDIDIER, P.—MORARI, M.: Interaction Measures for System under Decentralized Control, Automatica **22** No. 3 (1986), 309–319.

[12] DONDE, V.—PAI, A.—HISKENS, I. A.: Simulation and Optimization in a LFC System after Deregulation, IEEE Trans. On Power Systems **16** No. 3 (2001), 481–489.

[13] GAHINET, P.—NEMIROVSKI, A.—LAUB, A. J.—CHILALI, M.: LMI Control Toolbox, The MathWorks Inc., South Natick, 1995.

[14] SCHERER, C. W.: Multi-Objective Mixed H_2/H_∞ Control, IEEE Trans. on Automatic Control **40** No. 2 (1995), 1054-62.

[15] DJUKANOVIC, M. B.—KHAMMASH, M. H.—VITTAL, V.: Sensitivity Based Structured Singular Value Approach to Stability Robustness of Power Systems, IEEE Trans. On Power Systems **15** No. 2 (2000), 825–830.

[16] SHAYANFAR, H. A.—SHAYEGHI, H.: Decentralized Robust AGC Based on Structured Singular Values, J.Electrical Engineering **57** No. 6 (2006), 301-317.

[17] SKOGESTED, S.—POSTLETHWAITE, I.: Multivariable Feedback Control, John Wiley & Sons, 1996, pp. 449–467.

[18] SHAYEGHI, H.—KARRARI, M.: Theory of μ Synthesis for Power Systems Load Frequency Control, J. Electrical Engineering **51** No. 9-10 (2000), 258–263.

Received 3 March 2008

Hossein Shayeghi received the BS and MSE degrees in Electrical Engineering from KNT and Amirkabir Universities of Technology in 1996 and 1998, respectively and the Ph. D. degree in Electrical Engineering from Iran University of Science and Technology (IUST), Tehran, Iran, in 2006. Currently, He is an Assistant Professor at Technical Engineering Department of the University of Mohaghegh Ardabili, Ardabil, Iran. His research interests are in the application of Robust Control, Artificial Intelligence to Power System Control Design and restructuring. He is a member of Iranian Association of Electrical and Electronic Engineers (IAEEE) and IEEE.